Journal of Neuroscience Research

Journal of Neuroscience Research 89:117–126 (2011)

Small-Molecule Inhibitors of Bone Morphogenic Protein and Activin/Nodal Signals Promote Highly Efficient Neural Induction From Human Pluripotent Stem Cells

Asuka Morizane,[1,2] Daisuke Doi,[1,3] Tetsuhiro Kikuchi,[1,3] Kaneyasu Nishimura,[1,2] and Jun Takahashi[1,2,3]*

[1]Department of Biological Repair, Institute for Frontier Medical Sciences, Kyoto University, Kyoto, Japan
[2]Department of Cell Growth and Differentiation, Center for iPS Cell Research and Application, Kyoto University, Kyoto, Japan
[3]Department of Neurosurgery, Kyoto University Graduate School of Medicine, Kyoto, Japan

The balance of bone morphogenic protein (BMP), transforming growth factor-β (TGFβ)/activin/nodal, and Wnt signals regulates the early lineage segregation of human embryonic stem cells (ESCs). Here we demonstrate that a combination of small-molecule inhibitors of BMP (Dorsomorphin) and TGFβ/activin/nodal (SB431542) signals promotes highly efficient neural induction from both human ESCs and induced pluripotent stem cells (iPSCs). The combination of small molecules had effects on both cell survival and purity of neural differentiation, under conditions of stromal (PA6) cell coculture and feeder-free floating aggregation culture, for all seven pluripotent stem cell lines that we studied, including three ESC and four iPSC lines. Small molecule compounds are stable and cost effective, so our findings provide a promising strategy for controlled production of neurons in regenerative medicine.

Key words: small molecule; stromal cell-derived inducing activity; embryonic stem cell; induced pluripotent stem cell

Human embryonic stem cells (ESCs) or induced pluripotent stem cells (iPSCs) are promising potential sources of material for cell replacement therapy and arer useful experimental tools for in vitro models of human diseases (Soldner et al., 2009) and drug screening. Because these cells are pluripotent, it is critical for these purposes to control their differentiation toward a desired lineage. To generate neurons, human ESCs are often cultured on PA6 stromal feeder cells using stromal cell-derived inducing activity (SDIA; Kawasaki et al., 2000). Although this method efficiently generates neural cells from mouse ESCs, the effect on human ESCs is rather less, suggesting that additional factor might be needed.

Recent studies have revealed that a combination of signals from bone morphogenic protein (BMP), transforming growth factor-β (TGFβ)/activin/nodal, and Wnt regulates the lineage segregation of human ESCs (Wu et al., 2008; Murry and Keller, 2008; Xu et al., 2008). Inhibition of BMP and/or TGFβ/activin/nodal signals has been proposed to promote neural induction. Noggin binds BMP2, -4, and -7 with high affinity, consequently preventing ligation of their receptors, and is an effective inducer of neural cells from human ESCs (Ben-Hur et al., 2004; Pera et al., 2004; Chiba et al., 2008; Elkabetz et al., 2008; Chambers et al., 2009). A small-molecule compound, Dorsomorphin (6-[4-(2-piperidin-l-yl-ethoxy)phenyl]-3-pyridin-4-yl-pyrazolo[1,5-a]pyrimidine), also inhibits BMP signals by selective inhibition of the BMP type 1 receptors ALK2, ALK3, and ALK6, resulting in the reduction of SMAD1/5/8 phosphorylation (Yu et al., 2008). Dorsomorphin promotes neural induction from human ESCs (Wada et al., 2009) as well as cardiomyogenic differentiation of mouse ESCs (Hao et al., 2008). Another small-molecule compound, SB431542, inhibits TGFβ/activin/nodal signal by blocking phosphorylation of the ALK4, ALK5, and ALK7 receptors (Inman et al., 2002). SB431542 promotes

Additional Supporting Information may be found in the online version of this article.

Contract grant sponsor: Kobe Cluster Project; Contract grant sponsor: Project for Realization of Regenerative Medicine from the MEXT, Japan.

*Correspondence to: Jun Takahashi, MD, PhD, Department of Biological Repair, Institute for Frontier Medical Sciences, Kyoto University, 53 Shogoin Kawahara-cho, Sakyo-ku, Kyoto 606-8507, Japan. E-mail: jbtaka@frontier.kyoto-u.ac.jp

Received 12 April 2010; Revised 10 September 2010; Accepted 10 October 2010

Published online 8 December 2010 in Wiley Online Library (wileyonlinelibrary.com). DOI: 10.1002/jnr.22547

neural differentiation of human ESCs or iPSCs either by itself (Eiraku et al., 2008; Smith et al., 2008) or in combination with Noggin (Chambers et al., 2009). The combination of Dorsomorphin and SB431542, however, has never been tested.

The aim of this study was to compare the effect of Dorsomorphin, Noggin, and SB431542, either singly or in combination, on induction of neural lineages from human ESCs and iPSCs. To accomplish this, we cultured three human ESC lines and four iPSC lines on PA6 stromal feeder cells or as floating aggregates, induced them to differentiate in the presence of these molecules, and then evaluated their survival and differentiation toward neural or other lineages.

MATERIALS AND METHODS

Human ESC and iPSC Culture

Human ES cells (KhES-1, -2, -3; Suemori et al., 2006) were used in conformity with The Guidelines for Derivation and Utilization of Human Embryonic Stem Cells by the Ministry of Education, Culture, Sports, Science and Technology of Japan, after approval from the institutional review board. Undifferentiated human ESCs were maintained on a feeder layer of mouse embryonic fibroblasts (MEFs; inactivated with 10 μg/ml mitomycin C and seeded at 1.5×10^5 cells/10 cm dish) in DMEM/F12 (Sigma, St. Louis, MO) supplemented with 20% knockout serum replacement (KSR; Invitrogen, Carlsbad, CA), 5 ng/ml human fibroblast growth factor (FGF)-2 (Invitrogen), and 0.1 mM 2-mercaptoethanol. For passage, human ESC colonies were detached and recovered en bloc from the feeder layer by treatment with CTK dissociation solution (0.25% trypsin, 0.1% collagenase IV, 20% KSR, and 1mM $CaCl_2$ in PBS) at 37°C for 10 min. Human iPSCs (201B6, 201B7, 253G1, 253G4; Takahashi et al., 2007; Nakagawa et al., 2008) were maintained under the same conditions as ESCs except that STO feeder cells were used instead of MEFs. These cells were subjected to experiments between passages 20 and 40.

Differentiation on PA6 Stromal Feeder Cells

For differentiation, ESCs or iPSCs were broken into small cell clumps (10–20 cells) using CTK and plated at a density of $2–4 \times 10^5$ cells for a 10-cm dish or $2–4 \times 10^4$ cells/well for a 12-well plate on confluent PA6 feeder cells. Differentiation medium was as follows: DMEM/Ham'sF12 (Wako) supplemented with 5% KSR (Invitrogen), 2 mM L-glutamine (Sigma), and MEM nonessential amino acid solution (Invitrogen). To avoid apoptosis at the initial plating, we added 10 μM Y-276321 (ROCK inhibitor; Watanabe et al., 2007) in the first medium, which was replaced on day 7. Afterward, we changed medium every 3 days.

Differentiation by Feeder-Free Floating Aggregation Culture

As previously reported (Eiraku et al., 2008), 253G4 human iPS cells were dissociated to single cells and quickly reaggregated in 96-well low cell-adhesion plates (Lipidure-Coat Plate A-U96; NOF Corporation). For the first 4 days, the cells were cultured with or without Dorsomorphin and SB431542. On day 14, the cells were subjected to flow cytometric analyses with PSA-NCAM antibodies. For dopaminergic differentiation, we replated the cell aggregates in Dorsomorphin + SB431542 condition into a 60-mm Petri dish on day 14, then cultured them in Neurobasal medium containing B27 supplement (Invitrogen), 2 μM purmorphamine (Calbiochem, La Jolla, CA), and 100 ng/ml FGF8 (Peprotech). On day 28, the medium was replaced by Neurobasal medium supplemented with 2 ng/ml GDNF, 10 ng/ml BDNF (both from R&D Systems, Minneapolis, MN), 400 μM dbcAMP, and 200 μM ascorbic acid (both from Sigma-Aldrich). On day 35, the differentiated aggregates were fixed, frozen, and sliced with a cryostat at 10 μm thickness, then subjected to immunostaining.

Small Molecule Compounds

Dorsomorphin and SB431542 (both from Sigma-Aldrich) were dissolved in dimethylsulfoxide (DMSO). In a preliminary experiment, we tested four concentrations (20 nM, 200 nM, 2 μM, and 20 μM) for Dorsomorphin, and the best results were obtained at 2 μM. With regard to the concentration of SB431542, we chose 10 μM, which had been used in previous reports with human ESCs (Eiraku et al., 2008; Wu et al., 2008; Chambers et al., 2009). To compare with Dorsomorphin, we used Noggin at a concentration of 300 ng/ml according to the previous reports (Ben-Hur et al., 2004; Pera et al., 2004; Chiba et al., 2008; Elkabetz et al., 2008; Chambers et al., 2009).

Immunocytochemistry

Double-labeled immunohistochemical analyses were carried out after permeabilization (except for surface markers) and blocking with 0.3% Triton X-100 and 2% skim milk. Commercially available primary antibodies were purchased from Chemicon (Temecula, CA; human nestin/mouse monoclonal/1:500, PSA-NCAM/mouse monoclonal/1:100, SSEA3/rat monoclonal/1:50, tyrosine hydroxylase/mouse monoclonal/1:200, tyrosine hydroxylase/rabbit polyclonal/1:400), Babco (Berkeley, CA; β-tubulin III/rabbit polyclonal/1:1,000, Pax6/ rabbit polyclonal/1:200, TuJ1/mouse monolconal/1:1,000), BD Biosciences (San Kjose, CA; Oct-3/4/mouse monoclonal/1:300, SSEA4-PE conjugated/mouse monoclonal/1:5), Santa Cruz Biotechnology (Santa Cruz, CA; Oct3/4/rabbit polyclonal/1:500), R&D Systems (Nanog/goat polyclonal/1:200), Abcam (Cambridge, United Kingdom; cytokeratin/mouse monoclonal/1:40), and DakoCytomation (Glostrup, Denmark; human chorionic gonadotropin/rabbit polyclonal/1:600). The immunoreactive cells were visualized by using an Olympus IX71 microscope equipped with fluorescent filters (Olympus, Tokyo, Japan), a BioZero fluorescent microscope (Keyence, Osaka, Japan), and an FV1000D laser confocal microscope (Olympus). To figure out the percentage of immunopositive colonies, we counted different numbers of colonies, because cell viability differed with each condition (shown in Supp. Info. Table I).

Reverse Transcription-Polymerase Chain Reaction

Total RNA was extracted using an RNeasy Plus Mini kit (Qiagen, Valenica, VA), and reverse transcribed using a Super Script III First-Strand Synthesis System (Invitrogen). For PCR amplification, reactions were performed using Hot Star Taq (Qiagen) at 56°C. For semiquantitative PCR, reactions were optimized to allow for semiquantitative comparisons within the log phase of amplification. The primer sequences, product sizes, and cycle numbers are shown in Supporting Information Table II.

Flow Cytometry

All sorting procedures were carried out using FACS AriaII (BD Biosciences), and the data were analyzed using the FACSDiva software (BD Biosciences) and Flowjo flow cytometry analysis software (Tree Star, Inc.). Cells differentiated for 14 days were dissociated into a single-cell suspension using Accumax (Innovate Cell Technologies) and resuspended in PBS with with 2% fetal bovine serum (FBS), 20 mM D-glucose. We used the antibodies including PSA-NCAM, SSEA4-PE-conjugated nestin and Oct3/4. Dead cells were identified by using 7-aminoactionomycin-D (7AAD; BD Biosciences) staining and were excluded from analysis. We prepared cell suspensions of unstained cells, with PA6 cells as negative controls and undifferentiated ES cells as positive controls for the pluripotent markers to determine the threshold for detection of immunofluorescence. Because the culture was a mixture of ESC- or iPSC-derived and PA6 feeder cells, we estimated the number of ESC- or iPSC-derived cells by subtracting the number of simultaneously prepared PA6 cells in a separate 10-cm dish for each session. The average number of the feeder cells alone on day 14 was $51.2 \pm 14.9 \times 10^4$ (mean ± SD).

Western Blot Analyses

Human iPS cells (253G4) were differentiated on PA6 stromal feeder cells with or without Dorsomorphin and SB431542. On day 4, 50 ng/ml of BMP4 (R&D Systems) was added to the culture medium for 30 min, then lysed in CelLytic M buffer (Sigma-Aldrich). Total protein (10 μg) was electroporesed on 10% polyacrylamide gel and transferred onto the polyvinylidene difluoride membrane using the iBlot gel transfer system (Invitrogen). The membrane was probed with primary antibodies at 4°C overnight, followed by incubation with secondary antibody at room temperature for 1 hr, visualized using ECL plus substrate solution and detected with ImageQuant LAS 4000 (GE Healthcare, Piscataway, NJ). The following primary antibodies were used: SMAD 1/5/8 (Santa Cruz Biotechnology), SMAD 2/3, p-SMAD 1/5/8, p-SMAD 2/3 (Cell Signaling Technology, Danvers, MA), and β-actin (Sigma-Aldrich).

Statistical Analysis

Statistical analyses were performed using a commercially available software package (Prism 5; GraphPad, San Diego, CA). Immunocytochemistry data were analyzed by ANOVA followed by Dunnett's post hoc test. For the analyses of cell numbers using FACS, we used a paired *t*-test, and the values were compared with their controls. Data are presented as the means ± SEM or means ± SD. All results were derived from at least four independent experiments.

RESULTS

Both Dorsomorphin and SB431542 Promoted Survival of the Cells Derived From Pluripotent Stem Cells

The effect of Noggin, Dorsomorphin, and SB431542 on human ESCs and iPSCs was examined by culturing the cells on PA6 cells in the presence of these factors. It is possible that each human cell line has distinct propensity to differentiate (Osafune et al., 2008), so we investigated the survival and differentiation of the colonies derived from several cell lines, including three hESCs (KhES-1, -2, and -3) and four hiPSCs (253G1, 253G4, 201B6, and 201B7). Because cell morphologies were similar among the seven cell lines, the results from a representative cell line (253G4) are shown in Figure 1. Small clumps of cells proliferated and differentiated on the feeder and formed colonies after 14 days (Fig. 1A–D). In the presence of Dorsomorphin or Dorsomorphin + SB431542, the colonies were phase bright and compact, with clear margins. In contrast, in the presence of SB431542, flat cells extended from the core of the colonies. In the control condition (DMSO alone) and in the presence of Noggin, several colonies started to die and detached from the feeder in about 7 days. Although there were differences between cell lines, the number of surviving colonies on day 14 was increased by the addition of Dorsomorphin and SB431542 (Fig. 2B–H). When the results of all cell lines were combined, the increase was statistically significant (Fig. 2A), suggesting that these factors promoted the survival of the cells derived from pluripotent stem cells.

Dorsomorphin Supported Neural Differentiation

Previous reports (Zeng et al., 2004; Brederlau et al., 2006; Vazin et al., 2008) and our analysis with RT-PCR (Fig. 5B) showed that neural markers appeared after 7–14 days on PA6 cells, so we evaluated the neural differentiation on day 14 by immunocytochemistry, using early neural markers such as nestin, Pax6, and PSA-NCAM. At the same time, we also evaluated the remaining undifferentiated cells using pluripotent cell markers such as Oct3/4, Nanog, and SSEA3. Generally, the cells in the body of the compact colonies expressed nestin, and the cells in the margin expressed Oct3/4 (Fig. 1E–L). By double-labeled immunofluorescence, we quantified the percentages of colonies that contain $nestin^+$ or $Oct3/4^+$ cells. The combined results from all cell lines are presented in Figure 3A and those from each individual cell line in Figure 3B–H and Supporting Information Table I. In the presence of Dorsomorphin, ~60% of the colonies contained both neural and pluripotent cells (Figs. 1, 3), and the percentages of $nestin^+$ or $Oct3/4^+$ colonies were unchanged from the controls (Fig. 3). RT-PCR analysis confirmed that both

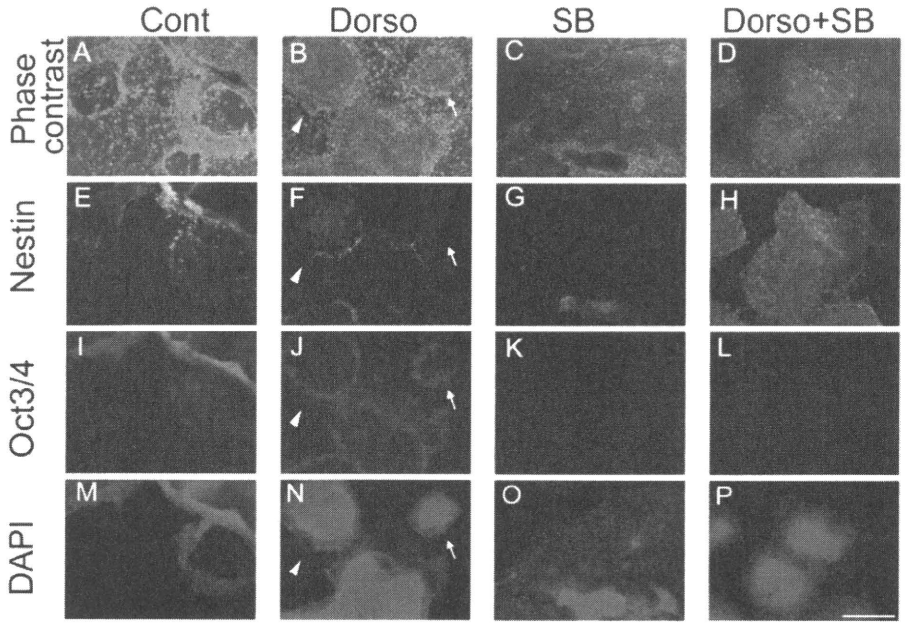

Fig. 1. Differentiation of human pluripotent stem cells under inhibition of BMP and/or activin/nodal signals. Phase-contrast images of the colonies derived from 253G4 cells on day 14 (**A–D**) and their immunocytochemistry of the same field for nestin (**E–H**), Oct3/4 (**I–L**), and DAPI (**M–P**) counterstaining. Arrowheads indicate colonies that contain both nestin$^+$ and Oct3/4$^+$ cells; arrows indicate Oct3/4$^+$/nestin$^-$ colonies. Scale bar = 500 μm.

early neural and pluripotent cells are present in the Dorsomorphin culture (Fig. 4I). Thus, Dorsomorphin by itself could enhance the survival of the ESCs and iPSCs and permissively support their neural commitment, but it did not initiate neural differentiation from the pluripotent state.

SB431542 Promoted Differentiation From the Pluripotent State

In contrast to Dorsomorphin, SB431542 treatment significantly decreased the percentage of Oct3/4$^+$ colonies, although that of nestin$^+$ colonies was unchanged (Figs. 1, 3). In the culture, we frequently observed large, flat cells, which expressed neither neural nor pluripotent markers (Fig. 1C,G,K,O). Instead, most of the cells were immunoreactive for cytokeratin, a marker for skin or extraembryonic tissue, and some for chorionic gonadtropin (CG), a marker for trophoblast (Fig. 4G,H). These flat colonies often contained a small number of compact nestin$^+$ cells in the core region (Fig. 1G). This region was so small that the actual number of nestin$^+$ cells seemed to be lower than estimated by the percentage of nestin$^+$ colonies. Our RT-PCR analysis revealed that expression of pluripotent markers was reduced by SB431542, whereas that of trophoblastic marker was increased (Fig. 4I). These results suggested that SB431542 promoted the ESCs and iPSCs to exit from the self-renewing state but not to differentiate into a neural lineage.

Combination of Dorsomorphin and SB431542 Promoted Neural Induction

Quantitative analysis of immunostained colonies with simultaneous administration of both Dorsomorphin and SB431542 revealed a significant increase of nestin$^+$ colonies and significant decrease of Oct3/4$^+$ colonies (Figs. 1D,H,L,P, 3). Most of the cells in these colonies were immunoreactive for the early neural markers nestin (Fig. 1H), Pax6 (Fig. 4C), and PSA-NCAM (Fig. 4F). Only a few cells were stained by pluripotent markers (Figs. 1L, 4C,F). RT-PCR analysis also showed that the cells with Dorsomorphin + SB431542 treatment expressed early neural markers but few pluripotent markers (Fig. 4I). Although there were some differences in differentiation propensity among cell lines under the control condition, the combination of Dorsomorphin and SB431542 could induce neural cells from all cell lines with high efficiency: more than 80% of nestin$^+$ colonies and less than 10% of Oct3/4$^+$ colonies, irrespective of the cell line (Fig. 3). These data suggest that simultaneous administration of these two small molecules promotes neural differentiation with high efficiency in this coculture system. In addition, Western blot analyses showed that the combination of Dorsomorphin and SB431542 reduced phosphorylation of both SMAD1/5/8 and SMAD2/3 in neural differentiation by SDIA (Fig. 4J).

Next, to determine whether the induced nestin$^+$ cells proceeded to differentiate into mature neurons afterward, we continued the differentiation culture of the iPSCs

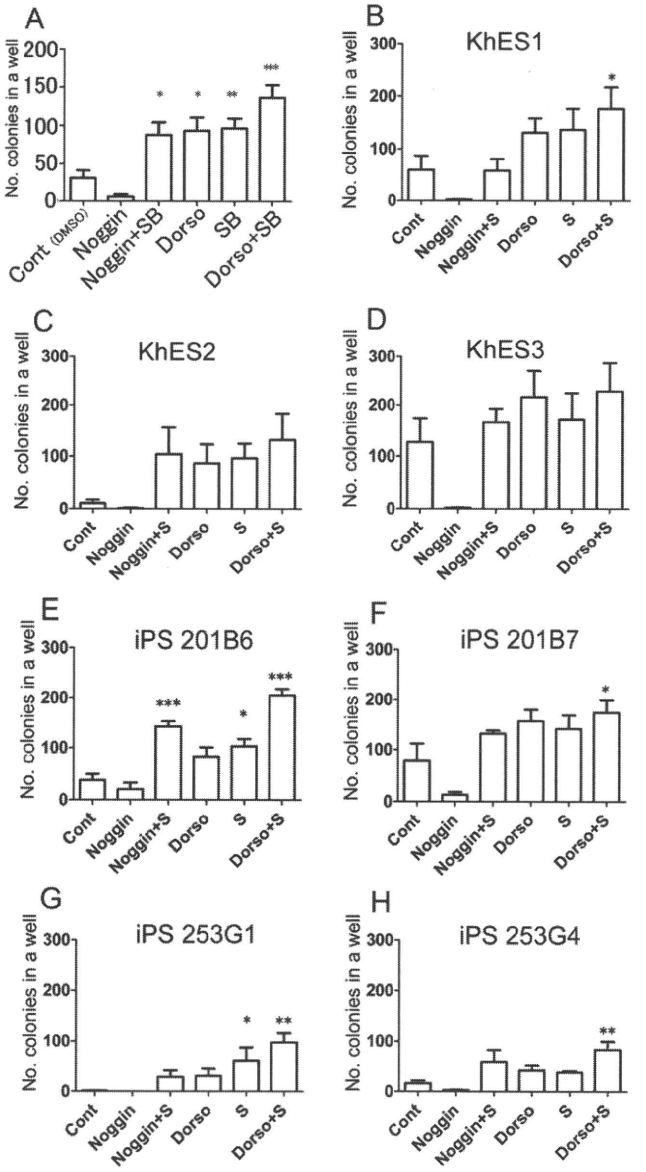

Fig. 2. Increase of the number of surviving colonies by the inhibition of BMP and/or activin/nodal signals. After differentiation for 14 days in a 12-well plate, the total number of surviving colonies was counted (n = 4 for each cell line). The numbers of colonies/well from the results of seven cell lines together (**A**) or each of them (**B–H**) are shown. Data are presented as the means ± SEM. Asterisks indicate statistical significance in comparison with the control (*$P < 0.05$, **$P < 0.005$, ***$P < 0.0005$).

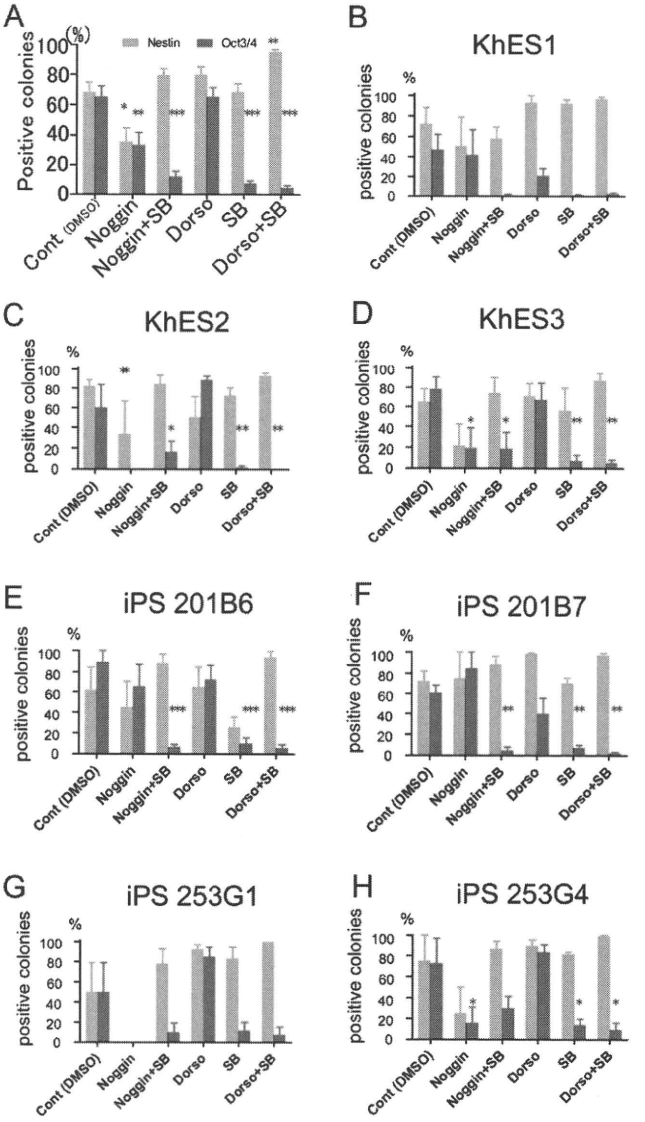

Fig. 3. Effect of the dual inhibition on the percentages of nestin$^+$ or Oct3/4$^+$ colonies. Double-labeled immunofluorescence study was performed on day 14, and the percentages of nestin$^+$ or Oct3/4$^+$ colonies were counted (n = 4 for each cell line). The percentages of nestin$^+$ or Oct3/4$^+$ colonies from the results of seven cell lines together (**A**) or each of them (**B–H**) are shown. Data are presented as the means ± SEM. Asterisks indicate statistical significance in comparison with the control (*$P < 0.05$, **$P < 0.005$, ***$P < 0.0005$).

(253G4) until day 21 in the presence of Dorsomorphin and SB431542. Because induction by SDIA generates mainly midbrain neurons (Kawasaki et al., 2000; Vazin et al., 2009), we focused on dopaminergic differentiation. On day 21, most of the cells exhibited neuronal morphology with long processes, and these cells were immunoreactive for both the pan-neuronal marker tubulin βIII (TubβIII), and the dopaminergic marker tyrosine hydroxylase (TH; Fig. 5A). RT-PCR analysis for temporal change of gene expression revealed that early neural markers, Sox1 and Pax6, appeared in 7 days. A set of markers for midbrain dopaminergic phenotypes, En1, Lmx1a, and TH, appeared by day 21 (Fig. 5B). These data suggested that coculture with PA6 stromal cells (SDIA method) in the presence of Dorsomorphin and SB431542 could generate mature dopaminergic neurons from human iPSCs.

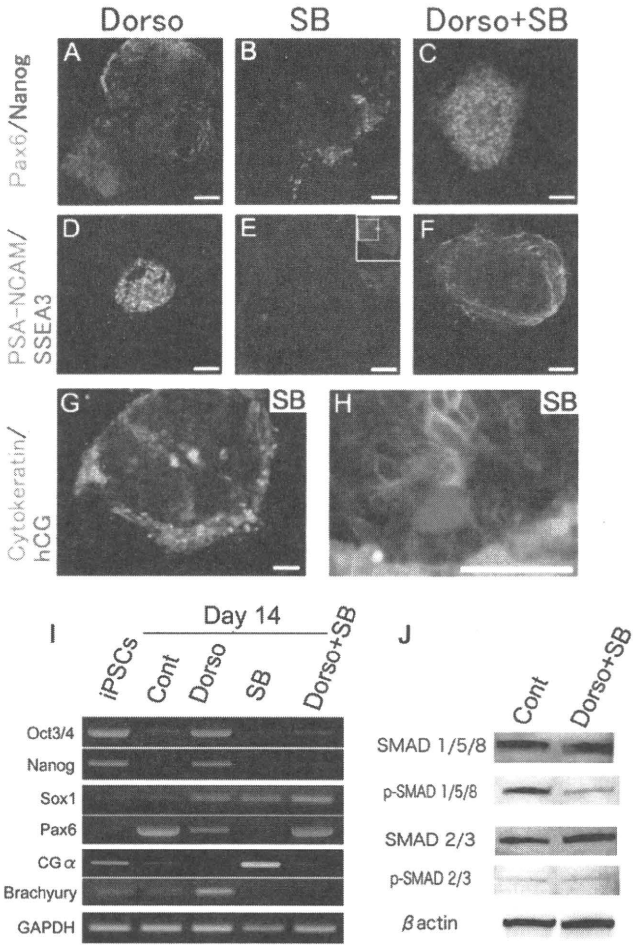

Fig. 4. Efficient neural induction by dual inhibition of BMP and activin/nodal signals. Double-labeled immunocytochemistry for Pax6 (green) and Nanog (red in **A–C**), PSA-NCAM (green) and SSEA3 (red in **D–F**), and cytokeratin (green) and hCG (red in **G,H**) of the 253G4-derived colonies differentiated in the presence of Dorsomorphin alone (Dorso; A,D), SB431542 alone (SB; B,E,G,H), and their combination (Dorso + SB; C,F). H is a higher magnification of G. **I**: RT-PCR analysis shows expression of neural markers (Sox1 and Pax6) in Dorso + SB, but almost absent for pluripotent (Oct3/4, Nanog), trophoblast (CGα), or mesoderm (brachyury) markers. **J**: Western blot analysis of 253G4 cells on PA6 cells at day 4, showing that phosphorylation of SMAD1/5/8 and SMAD2/3 was reduced in the presence of Dorsomorphin and SB431542. Scale bars = 100 μm.

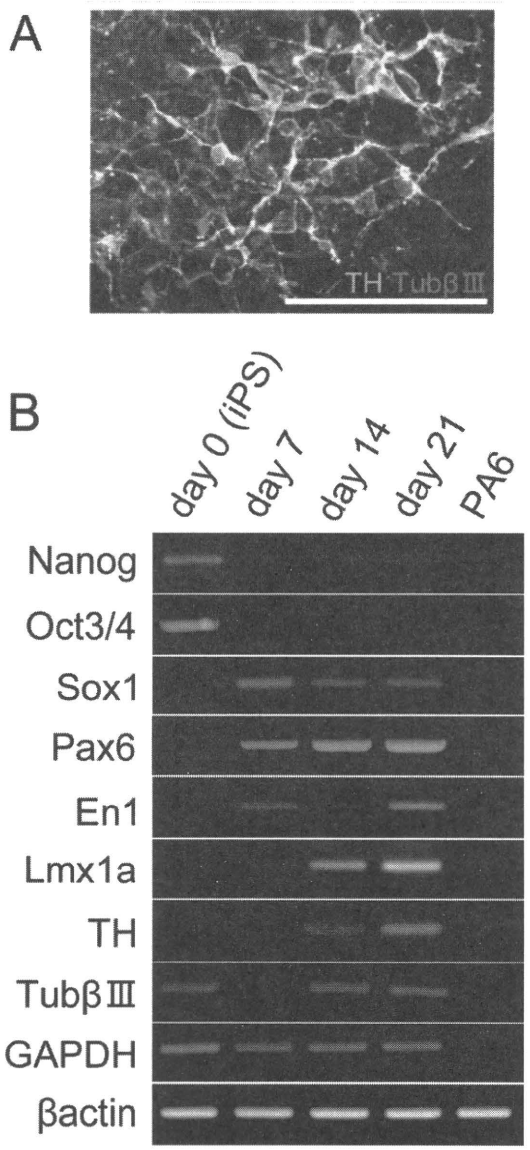

Fig. 5. Neuronal maturation of hiPSCs under dual inhibition. **A**: Immunocytochemistry of 253G4 cells treated by both Dorsomorphin and SB431542 for 21 days revealed generation of dopaminergic neurons (green = TubβIII, red = TH). **B**: RT-PCR analysis shows temporal changes in the expression of pluripotent (Nanog, Oct3/4), neural progenitor (Sox1, Pax6), neuronal (TubβIII), and dopaminergic (Lmx1a, En1, and TH) markers during the differentiation. The primers for GAPDH were human specific. Scale bar = 100 μm.

Dorsomorphin and SB431542 Increased Absolute Number of Neural Cells

The combination of Dorsomorphin and SB431542 notably increased the percentage of nestin$^+$ colonies and reduced the percentage of Oct3/4$^+$ colonies. For a further analysis, we quantified the number of nestin$^+$ or Oct3/4$^+$ cells in the culture of human iPSCs (201B7) on day 14 by flow cytometry. The histograms of nestin$^+$ or Oct3/4$^+$ cells showed a biphasic distribution in the control culture (Fig. 6A, top) where the percentages were 16.2% ± 1.8% and 6.7% ± 11.9% of the total iPSC-derived cells, respectively (n = 4). In contrast, in adding both Dorsomorphin and SB431542, the cell distribution became more monophagic, and the percentages of nestin$^+$ and Oct3/4$^+$ cells were 88.0% ± 7.9% and 0.6% ± 1.1%, respectively (n = 4; Fig. 6A, bottom). In

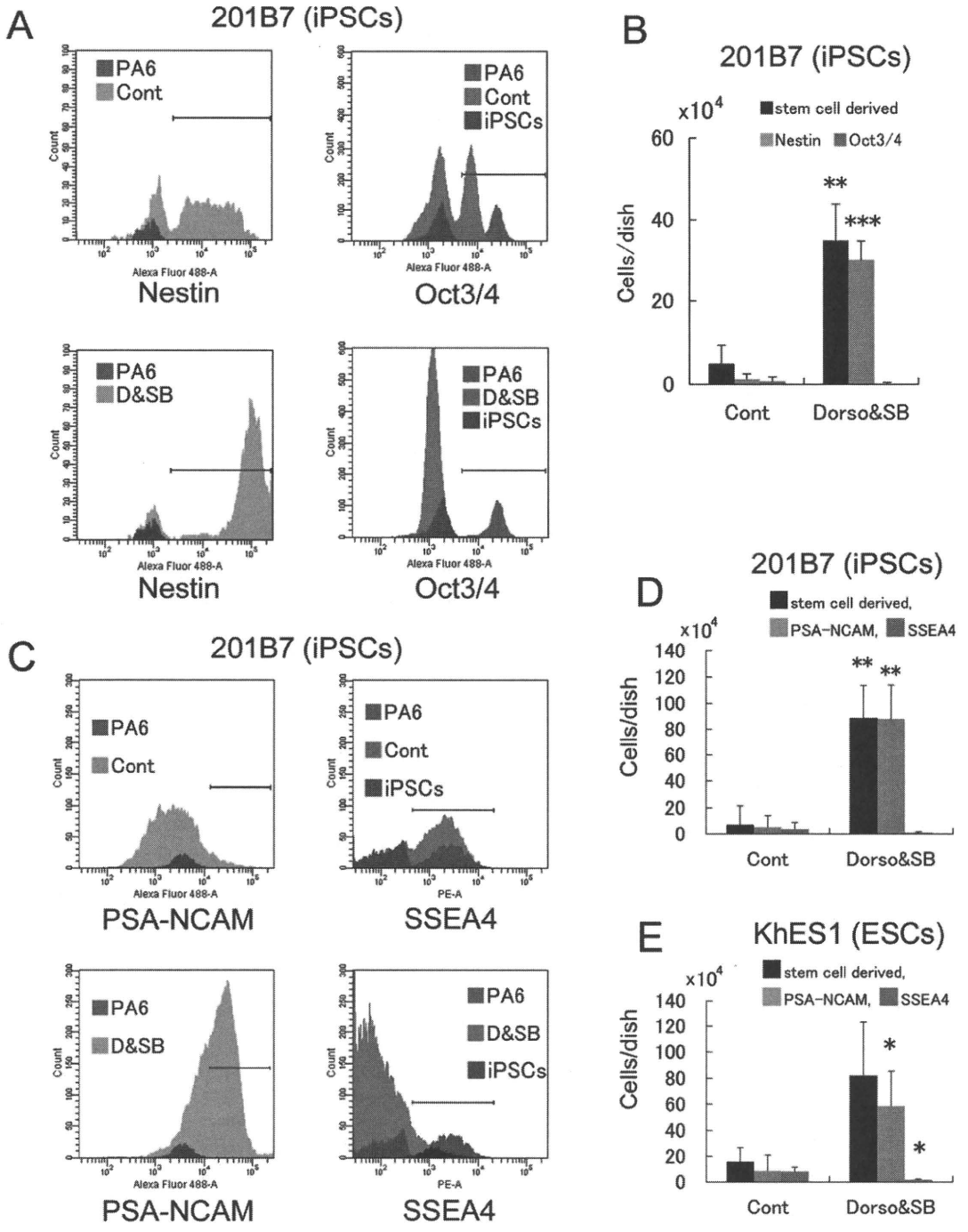

Fig. 6. Increase of absolute number of induced neural cells by dual inhibition. **A,C**: Flow cytometric profiles of 201B7 cells differentiated for 14 days without (Cont) or with (D&SB) Dorsomorphin and SB431542. The results of PA6 cells (negative control) or undifferentiated 201B7 cells (positive control for Oct3/4) are superimposed. **B,D**: Absolute number of the 201B7 cell-derived (total cell number – number of PA6 cells, black), nestin$^+$ (green), or Oct3/4$^+$ (red) cells per 10-cm dish. **E**: Absolute number of the KhES-1 cell-derived, nestin$^+$, or Oct3/4$^+$ cells per 10-cm dish. Data are presented as the means ± SD. Asterisks indicate statistical significance in comparison with the control (n = 4; $*P < 0.05$, $**P < 0.005$, $***P < 0.0005$).

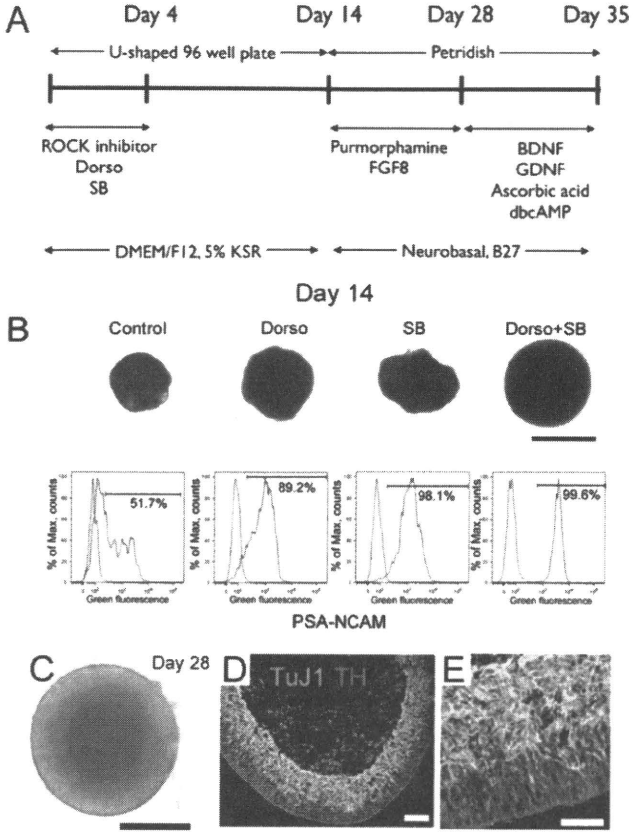

Fig. 7. Efficient neural induction by dual inhibition in a feeder-free culture. **A**: Protocol for generating dopaminergic neurons by feeder-free floating aggregation culture. **B**: Phase-contrast images of representative aggregates by 253G4 cells (top), and histograms of flow cytometry with PSA-NCAM antibody (blue line; bottom) after 14 days of differentiation. Red line: negative control stained with secondary antibodies only. **C**: Phase-contrast image of an aggregate at day 28. **D,E**: Immunofluorescence images of a sliced aggregate at day 35, showing $TuJ1^+$ (green) and TH^+ (red) cells in the outer layer. Scale bars = 500 μm in B,C; 100 μm in D; 50 μm in E.

addition, consistently with the result in Figure 2A, the treatment with Dorsomorphin and SB431542 supported the survival of iPSC-derived cells (Fig. 6B). As a result, the absolute number of $nestin^+$ cells increased by 25.0 times compared with the control condition, whereas $Oct3/4^+$ cells almost disappeared.

Next, we used other markers, PSA-NCAM and SSEA4, for neural and pluripotent cells, respectively (Fig. 6C–E, Supp. Info. Fig. 1). These are cell surface markers with the potential to be used for sorting donor cells in transplantation. Once again, flow cytometry demonstrated the effective neural induction by Dorsomorphin and SB431542 in both human iPSCs (201B7) and ESCs (KhES-1). In case of B7 cells, the percentages of $PSA\text{-}NCAM^+$ cells increased from 53.7% ± 29.4% to 98.6% ± 6.9%. In contrast, the percentages of $SSEA4^+$ cells decreased from 52.3% ± 17% to 1.2% ± 1.5% (n = 4; Fig. 6C). Similarly, in the case of KhES-1 cells, the percentage of $PSA\text{-}NCAM^+$ cells increased from 52.4% ± 61.5% to 80.8% ± 34.4%, whereas the percentage of $SSEA4^+$ cells decreased from 31.1% ± 3.5% to 2.6% ± 1.4% (n = 4). The absolute number of $PSA\text{-}NCAM^+$ cells increased by 16.8 times and 6.7 times for 201B7 and KhES-1, respectively (Fig. 6D,E). We also performed flow cytometry analyses with PSA-NCAM antibodies for all seven pluripotent cell lines. By setting proper gates in the dot plot of FSC-A vs. SSC-A to exclude the feeder and dead cells, the analyses showed that more than 90% of the cells were positive for PSA-NCAM (Supp. Info. Fig. 1). Taken together, our results demonstrate that the combination of Dorsomorphin and SB431542 significantly promotes neural induction, by increasing both the purity of the culture and the absolute number of neural cells generated.

Dorsomoprhin and SB431542 Also Works in Feeder-Free Neural Induction

To determine whether the combination of Dorsomorphin and SB431542 has a direct effect on pluripotent cells, we next applied this combination to another neural induction method: a feeder-free floating aggregation culture (Eiraku et al., 2008). We added the inhibitors for the first 4 days of differentiation from the beginning of single cell culture (Fig. 7A). On day 14, cell aggregates in the Dorsomorphin + SB431542 condition were round, with clear margins, whereas control aggregates with vehicle (DMSO) were fragile, and, even when they formed aggregates, they were rough with heterogeneous cell components. Furthermore, flow cytometry analyses revealed that the combination of Dorsomorphin and SB431542 increased the percentage of $PSA\text{-}NCAM^+$ cells in the aggregates (Fig. 7B). These results suggest that addition of these two small molecules promotes neural induction through direct effect on human pluripotent cells.

For further differentiation of the dopaminergic phenotype, we continued the floating culture as shown in Figure 7A. By day 28, the the aggregates had become larger than 1 mm in diameter (Fig. 7C). On day 35, the outer layer of the aggregates consisted of $TuJ1^+$ neurons and most of them also expressed TH, suggesting that this feeder-free floating aggregation culture with Dorsomorphin and SB431542 could efficiently generate dopaminergic neurons.

DISCUSSION

Our results clearly show that simultaneous administration of Dorsomorphin and SB431542 efficiently enhances the neural induction of human ESCs and iPSCs. In neural differentiation from pluripotent stem cells, the following steps are involved: 1) exit from the pluripotent state, 2) differentiation into the lineages of embryonic tissues instead of extraembryonic tissues, 3) differentiation into ectoderm instead of primitive streak, and 4) differentiation into neural cells instead of epidermal cells. Regarding the normal embryonic development

or differentiation of pluripotent stem cells, TGFβ/activin/nodal signals have multiple effects in each step of the differentiation. Because the TGFβ/activin/nodal signal maintains the pluripotency of hESCs, inhibition of this signal results in induction of differentiation (James et al., 2005). The signal of BMP4 initiates differentiation into trophoblasts (Xu et al., 2002) or extraembryonic tissue (Conley et al., 2007), whereas nodal has an inhibitory effect on this step. Previous reports showed that blocking the nodal signal with SB431542 promotes trophoblast differentiation of ESCs (Munir et al., 2004; Wu et al., 2008; Chambers et al., 2009). Consistent with those reports, our results show that SB431542 by itself reduced the number of $Oct3/4^+$ colonies but increased the number of flat trophoblast-like cells (Fig. 1C) and hCG^+ cells (Fig. 4G–I). The TGFβ/activin/nodal signal also induces primitive streak rather than ectoderm. Inhibition of this signal cascade leads to neural induction from hESCs (Eiraku et al., 2008; Smith et al., 2008; Chambers et al., 2009). In this step, BMP signal, as well as Wnt and activin signals, blocks ectodermal differentiation and promotes the development of primitive streak (Sumi et al., 2008). After ectodermal differentiation, BMP4 blocks neural differentiation and promotes epidermal development (Wilson and Hemmati-Brivanlou, 1995). Thus, inhibition of BMP signal promotes neural differentiation but, at the same time, maintains pluripotency of the cells (Xu et al., 2005). Taking these results into account, one can expect that the dual inhibition of the two signals might work together to cause more efficient neural induction. This hypothesis was proved to be true by a recent study using Noggin (instead of Dorsomorphin) and SB431542 in an adherent culture system (Chambers et al., 2009) as well as by the present study. We further demonstrated that Dorsomorphin works better than Noggin in seven hESC or hiPSC lines and also that the dual inhibition increases the absolute number of the induced neural cells. It remains to be determined why Dorsomorphin, SB431542, and their combination enhance colony survival. Small colonies were formed in a couple of days, but, without these factors, some of them started to die and detach from the feeder layer. Considering that both neural cells and undifferentiated ESCs can survive on PA6 cells, it is possible that the dead cells were differentiated into the other lineages that could not survive under our coculture conditions.

In this study, Dorsomorphin supported colony survival, but Noggin failed to do so. This discrepancy between Noggin and Dorsomorphin is also observed in a floating-culture system without PA6 cells (T.K., A.M., D.D., J.T. unpublished data) and in cardiomyogenic differentiation (Hao et al., 2008). Recently another group has also reported a promoting effect of Dorsomorphin and SB431542 on neural induction from human pluripotent cells, where they formed embryoid bodies (Kim et al., 2010). Interestingly, the authors also pointed out a more drastic effect of Dorsomorphin than of Noggin in their study. These distinct effects may reflect intrinsic differences between the small molecule Dorsomorphin and a protein-based BMP antagonist. It is possible that the small molecule more easily penetrates multiple cell layers within colonies. The differences could also arise from their molecular mechanisms: Noggin inhibits BMP4-induced phosphorylation of both SMAD1/5/8 and MAPK p38, whereas Dorsomorphin inhibits SMAD1/5/8 selectively (Yu et al., 2008). In addition, Dorsomorphin has several advantages. First, it is more than 100 times less expensive than protein-based BMP antagonists. Second, Dorsomorphin has less interbatch variability. Insofar as Noggin is a recombinant protein, variance among product batches cannot be avoided. Third, in clinical applications, the risk of infection and immunoreaction would be lower for small molecules than for recombinant proteins.

We did not find any apparent differences between human ESCs and iPSCs with regard to their propensity to differentiate. Among seven cell lines, however, we observed some differences under the control conditions, as previously reported (Osafune et al., 2008). All iPSC lines that we used in this study originated from the same skin tissue, meaning that their original genetic backgrounds were identical. 201B6 and 201B7 cells were generated by introducing four transcriptional factors, Oct3/4, Klf4, c-Myc, and Sox2 (Takahashi et al., 2007), whereas 253G1 and 253G4 were generated by three factors without c-Myc (Nakagawa et al., 2008). The difference in the integration site might cause some of the discrepancies. It has been reported that mouse iPS cells have variation in their neural differentiation capacity and teratoma-forming propensity after transplantation (Miura et al., 2009). Some cell lines contain differentiation-resistant cells that kept expression of pluripotent markers such as Nanog through a conventional differentiation protocol. Overall, it seems that both ESCs and iPSCs have variations in differentiation propensities between cell lines. Nevertheless, simultaneous addition of Dorsomorphin and SB431542 could repress those different propensities of cell lines, at least the seven cell lines that we examined (Fig. 3, Supp. Info. Fig.1). Furthermore, the absolute number of induced neural cells increased by 25 times in 14 days (Fig. 6B,D,E).

In conclusion, a combination of Dorsomorphin and SB431542 efficiently enhances neural induction from both human ECSs and human iPSCs under conditions of stromal cell coculture and feeder-free floating aggregation culture. These small molecules have advantages because they provide stable and low-cost culture systems. Our results will contribute to clinical applications of human pluripotent stem cells as donor cells for transplantation or as in vitro models of human diseases.

ACKNOWLEDGMENTS

We thank Dr. H. Suemori for providing human ESCs and Dr. S. Yamanaka for human iPSCs. We also thank M. Katsukawa and K. Kubota for their technical assistance and other members of the laboratory.

REFERENCES

Ben-Hur T, Idelson M, Khaner H, Pera M, Reinhartz E, Itzik A, Reubinoff BE. 2004. Transplantation of human embryonic stem cell-derived neural progenitors improves behavioral deficit in parkinsonian rats. Stem Cells 22:1246–1255.

Brederlau A, Correia AS, Anisimov SV, Elmi M, Paul G, Roybon L, Morizane A, Bergquist F, Riebe I, Nannmark U, Carta M, Hanse E, Takahashi J, Sasai Y, Funa K, Brundin P, Eriksson PS, Li JY. 2006. Transplantation of human embryonic stem cell-derived cells to a rat model of Parkinson's disease: effect of in vitro differentiation on graft survival and teratoma formation. Stem Cells 24:1433–1440.

Chambers SM, Fasano CA, Papapetrou EP, Tomishima M, Sadelain M, Studer L. 2009. Highly efficient neural conversion of human ES and iPS cells by dual inhibition of SMAD signaling. Nat Biotechnol 27:275–280.

Chiba S, Lee YM, Zhou W, Freed CR. 2008. Noggin enhances dopamine neuron production from human embryonic stem cells and improves behavioral outcome after transplantation into parkinsonian rats. Stem Cells 26:2810–2820.

Conley BJ, Ellis S, Gulluyan L, Mollard R. 2007. BMPs regulate differentiation of a putative visceral endoderm layer within human embryonic stem-cell-derived embryoid bodies. Biochem Cell Biol 85:121–132.

Eiraku M, Watanabe K, Matsuo-Takasaki M, Kawada M, Yonemura S, Matsumura M, Wataya T, Nishiyama A, Muguruma K, Sasai Y. 2008. Self-organized formation of polarized cortical tissues from ESCs and its active manipulation by extrinsic signals. Cell Stem Cell 3:519–532.

Elkabetz Y, Panagiotakos G, Al Shamy G, Socci ND, Tabar V, Studer L. 2008. Human ES cell-derived neural rosettes reveal a functionally distinct early neural stem cell stage. Genes Dev 22:152–165.

Hao J, Daleo MA, Murphy CK, Yu PB, Ho JN, Hu J, Peterson RT, Hatzopoulos AK, Hong CC. 2008. Dorsomorphin, a selective small molecule inhibitor of BMP signaling, promotes cardiomyogenesis in embryonic stem cells. PLoS One 3:e2904.

Inman GJ, Nicolás FJ, Callahan JF, Harling JD, Gaster LM, Reith AD, Laping NJ, Hill CS. 2002. SB-431542 is a potent and specific inhibitor of transforming growth factor-beta superfamily type I activin receptor-like kinase (ALK) receptors ALK4, ALK5, and ALK7. Mol Pharmacol 62:65–74.

James D, Levine AJ, Besser D, Hemmati-Brivanlou A. 2005. TGFbeta/activin/nodal signaling is necessary for the maintenance of pluripotency in human embryonic stem cells. Development 132:1273–1282.

Kawasaki H, Mizuseki K, Nishikawa S, Kaneko S, Kuwana Y, Nakanishi S, Nishikawa SI, Sasai Y. 2000. Induction of midbrain dopaminergic neurons from ES cells by stromal cell-derived inducing activity. Neuron 28:31–40.

Kim DS, Lee JS, Leem JW, Huh YJ, Kim JY, Kim HS, Park IH, Daley GQ, Hwang DY, Kim DW. 2010. Robust enhancement of neural differentiation from human ES and iPS cells regardless of their innate difference in differentiation propensity. Stem Cell Rev 6:270–281.

Miura K, Okada Y, Aoi T, Okada A, Takahashi K, Okita K, Nakagawa M, Koyanagi M, Tanabe K, Ohnuki M, Ogawa D, Ikeda E, Okano H, Yamanaka S. 2009. Variation in the safety of induced pluripotent stem cell lines. Nat Biotechnol 27:743–745.

Munir S, Xu G, Wu Y, Yang B, Lala PK, Peng C. 2004. Nodal and ALK7 inhibit proliferation and induce apoptosis in human trophoblast cells. J Biol Chem 279:31277–31286.

Murry CE, Keller G. 2008. Differentiation of embryonic stem cells to clinically relevant populations: lessons from embryonic development. Cell 132:661–680.

Nakagawa M, Koyanagi M, Tanabe K, Takahashi K, Ichisaka T, Aoi T, Okita K, Mochiduki Y, Takizawa N, Yamanaka S. 2008. Generation of induced pluripotent stem cells without Myc from mouse and human fibroblasts. Nat Biotechnol 26:101–106.

Osafune K, Caron L, Borowiak M, Martinez RJ, Fitz-Gerald CS, Sato Y, Cowan CA, Chien KR, Melton DA. 2008. Marked differences in differentiation propensity among human embryonic stem cell lines. Nat Biotechnol 26:313–315.

Pera MF, Andrade J, Houssami S, Reubinoff B, Trounson A, Stanley EG, Ward-van Oostwaard D, Mummery C. 2004. Regulation of human embryonic stem cell differentiation by BMP-2 and its antagonist Noggin. J Cell Sci 117:1269–1280.

Smith JR, Vallier L, Lupo G, Alexander M, Harris WA, Pedersen RA. 2008. Inhibition of activin/nodal signaling promotes specification of human embryonic stem cells into neuroectoderm. Dev Biol 313:107–117.

Soldner F, Hockemeyer D, Beard C, Gao Q, Bell GW, Cook EG, Hargus G, Blak A, Cooper O, Mitalipova M, Isacson O, Jaenisch R. 2009. Parkinson's disease patient-derived induced pluripotent stem cells free of viral reprogramming factors. Cell 136:964–977.

Suemori H, Yasuchika K, Hasegawa K, Fujioka T, Tsuneyoshi N, Nakatsuji N. 2006. Efficient establishment of human embryonic stem cell lines and long-term maintenance with stable karyotype by enzymatic bulk passage. Biochem Biophys Res Commun 345:926–932.

Sumi T, Tsuneyoshi N, Nakatsuji N, Suemori H. 2008. Defining early lineage specification of human embryonic stem cells by the orchestrated balance of canonical Wnt/beta-catenin, activin/nodal and BMP signaling. Development 135:2969–2979.

Takahashi K, Tanabe K, Ohnuki M, Narita M, Ichisaka T, Tomoda K, Yamanaka S. 2007. Induction of pluripotent stem cells from adult human fibroblasts by defined factors. Cell 131:861–872.

Vazin T, Chen J, Lee CT, Amable R, Freed WJ. 2008. Assessment of stromal-derived inducing activity in the generation of dopaminergic neurons from human embryonic stem cells. Stem Cells 26:1517–1525.

Vazin T, Becker KG, Chen J, Spivak CE, Lupica CR, Zhang Y, Worden L, Freed WJ. 2009. A novel combination of factors, termed SPIE, which promotes dopaminergic neuron differentiation from human embryonic stem cells. PLoS One 4:e6606.

Wada T, Honda M, Minami I, Tooi N, Amagai Y, Nakatsuji N. 2009. Highly efficient differentiation and enrichment of spinal motor neurons derived from human and monkey embryonic stem cells. PLoS One 4:e6722.

Watanabe K, Ueno M, Kamiya D, Nishiyama A, Matsumura M, Wataya T, Takahashi JB, Nishikawa S, Nishikawa S, Muguruma K, Sasai Y. 2007. A ROCK inhibitor permits survival of dissociated human embryonic stem cells. Nat Biotechnol 25:681–686.

Wilson PA, Hemmati-Brivanlou A. 1995. Induction of epidermis and inhibition of neural fate by Bmp-4. Nature 376:331–333.

Wu Z, Zhang W, Chen G, Cheng L, Liao J, Jia N, Gao Y, Dai H, Yuan J, Cheng L, Xiao L. 2008. Combinatorial signals of activin/nodal and bone morphogenic protein regulate the early lineage segregation of human embryonic stem cells. J Biol Chem 283:24991–25002.

Xu RH, Chen X, Li DS, Li R, Addicks GC, Glennon C, Zwaka TP, Thomson JA. 2002. BMP4 initiates human embryonic stem cell differentiation to trophoblast. Nat Biotechnol 20:1261–1264.

Xu RH, Peck RM, Li DS, Feng X, Ludwig T, Thomson JA. 2005. Basic FGF and suppression of BMP signaling sustain undifferentiated proliferation of human ES cells. Nat Methods 2:185–190.

Xu RH, Sampsell-Barron TL, Gu F, Root S, Peck RM, Pan G, Yu J, Antosiewicz-Bourget J, Tian S, Stewart R, Thomson JA. 2008. NANOG is a direct target of TGFbeta/activin-mediated SMAD signaling in human ESCs. Cell Stem Cell 3:196–206.

Yu PB, Hong CC, Sachidanandan C, Babitt JL, Deng DY, Hoyng SA, Lin HY, Bloch KD, Peterson RT. 2008. Dorsomorphin inhibits BMP signals required for embryogenesis and iron metabolism. Nat Chem Biol 4:33–41.

Zeng X, Cai J, Chen J, Luo Y, You ZB, Fotter E, Wang Y, Harvey B, Miura T, Backman C, Chen GJ, Rao MS, Freed WJ. 2004. Dopaminergic differentiation of human embryonic stem cells. Stem Cells 22:925–940.

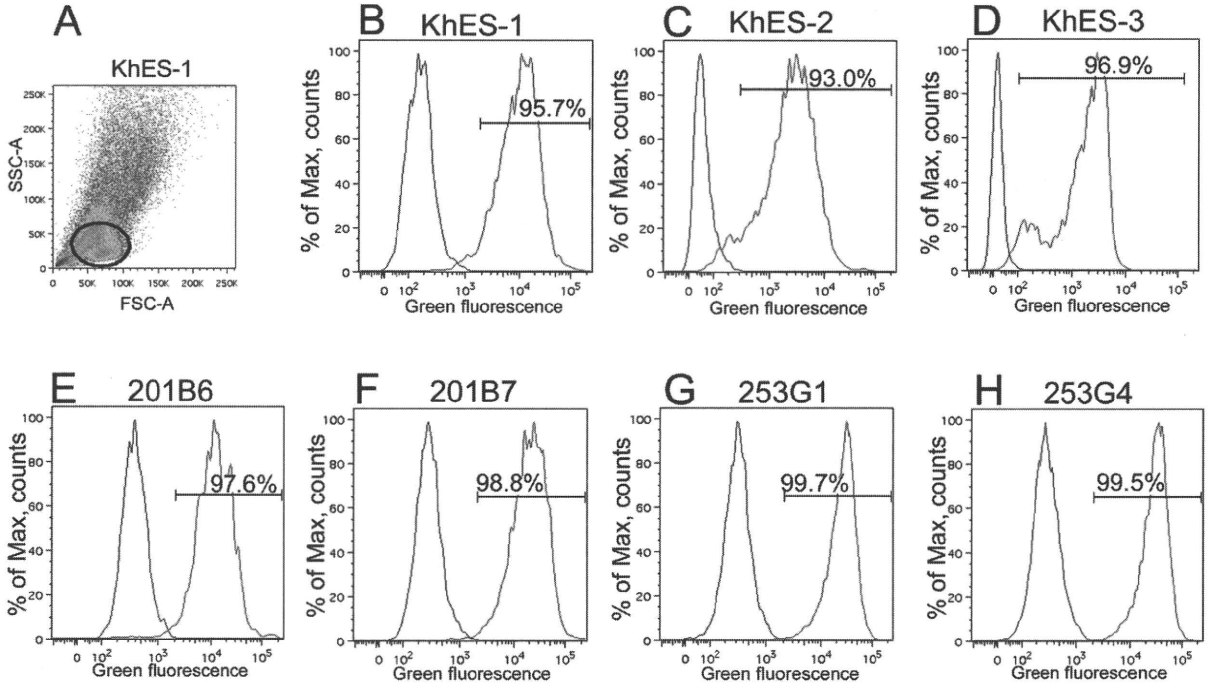
A
KhES-1
SSC-A
FSC-A
B KhES-1
95.7%
C KhES-2
93.0%
D KhES-3
96.9%
E 201B6
97.6%
F 201B7
98.8%
G 253G1
99.7%
H 253G4
99.5%
% of Max, counts
Green fluorescence

Suppl. TABLE I Mean numbers of colonies counted for Figure 3

		Control	Noggin	Noggin+SB	Dorso [a)]	SB [b)]	Dorso+SB
KhES1							
	Nestin	19.1	1.6	12.3	55.1	50.6	77.0
	Oct3/4	12.4	1.4	0.2	12.2	0.6	1.9
	Total	**26.5**	**3.25**	**21.25**	**59.25**	**55.0**	**79.75**
KhES2							
	Nestin	4.8	0.0	32.4	20.6	38.6	56.0
	Oct3/4	3.8	0.0	9.8	29.4	1.8	0.0
	Total	**5.75**	**0.5**	**39.75**	**33.75**	**53.75**	**56.75**
KhES3							
	Nestin	28.7	0.0	34.9	47.2	27.1	67.1
	Oct3/4	27.5	0.0	9.8	51.9	3.6	2.2
	Total	**39**	**1.25**	**45.25**	**67**	**36.5**	**74.75**
201B6							
	Nestin	9.9	3.8	26.8	14.6	6.1	42.8
	Oct3/4	14.3	5.5	1.9	16.3	2.4	2.6
	Total	**16**	**8.5**	**30.25**	**22.5**	**24**	**45.5**
201B7							
	Nestin	17.1	4.8	36.6	37.2	21.4	46.5
	Oct3/4	13.6	5.8	1.7	16.9	2.1	1.4
	Total	**23.25**	**7.25**	**38**	**37.5**	**28.75**	**48.25**
253G1							
	Nestin	0.3	0.0	8.3	9.3	14.3	17.5
	Oct3/4	0.3	0.0	1.0	8.5	2.0	1.3
	Total	**0.5**	**0.0**	**10.75**	**10**	**17.25**	**17.5**
253G4							
	Nestin	4.3	0.7	18.1	13.8	11.0	24.2
	Oct3/4	4.1	0.4	7.3	13.0	2.1	2.8
	Total	**6.5**	**2.0**	**19.75**	**14.75**	**13.75**	**24.5**

a) Dorso: Dorsomorphin, b) SB: SB431542

We performed four independent experiments for all cell lines and the mean numbers in each experiment are listed. Because only small number of colonies survived in some conditions such as Control (DMSO) and Noggin only, the numbers of counted colonies varied between conditions.

Suppl. TABLE II Primers used for RT-PCR

Gene	Primer sequence (fw)	Primer sequence (rv)	Product size (bp)	Cycle No.
Oct3/4	AGAAGGATGTGGTCCGAGTGTG	CCACCCTTTGTGTTCCCAATTCC	408	28
Nanog	AACTGCATGCAGGACTGCAGAG	TGAACCTCAGCTACAAACAGGTG	367	28
Pax6	GCCCTGGAGAAAGAGTTTGAGAGAACCCATT	GGGGAAATGAGTCCTGTTGAAGTGGTGC	527	32
Sox1	CACAACTCGGAGATCAGCAA	GTCCTTCTTGAGCAGCGTCT	171	32
TubβIII	GGAGATCGTGCACATCCAG	GAGGCCTCGTTGTAGTAGACG	159	28
En1	ACTTATGGGCTCAGCCAACG	TAGCGGTTTGCCTGGAACTC	228	32
Lmx1a	GATCCCTTCCGACAGGGTCTC	GGTTTCCCACTCTGGACTGC	177	32
TH	TCATCACCTGGTCACCAAGTT	GGTCGCCGTGCCTGTACT	125	32
CGα	CAACCGCCCTGAACACATCC	CAGCAAGTGGACTCTGAGGTG	298	32
Brachyury	AATTGGTCCAGCCTTGGAAT	CGTTGCTCACAGACCACA	112	32
GAPDH (human)	GGTCGGAGTCAACGGATTTG	TCAGCCTTGACGGTGCCATG	174	28
β-actin (mouse)	GACCCAGATCATGTTTGAGACC	GAGAGCATAGCCCTCGTAGA	157	32

TubβIII: tublin beta III; En1: Engrailed 1; TH: Tyrosine hydroxylase; CGα: chorionic gonadotropin alpha; GAPDH: Glyceraldehyde-3-phosphate dehydrogenase

The PCR conditions were as follows: 95°C /5 minutes, 94°C /30 seconds, 56°C / 30 seconds, 72°C /1 minute, 72°C /10 minutes.

Journal of Neuroscience Research

Journal of Neuroscience Research 88:542–551 (2010)

Matrigel Supports Survival and Neuronal Differentiation of Grafted Embryonic Stem Cell-Derived Neural Precursor Cells

Makoto Uemura,[1] Mohamed M. Refaat,[2,3] Mizuya Shinoyama,[2] Hideki Hayashi,[1,2] Nobuo Hashimoto,[2] and Jun Takahashi[1,2]*

[1]Department of Biological Repair, Institute for Frontier Medical Sciences, Kyoto University, Kyoto, Japan
[2]Department of Neurosurgery, Kyoto University Graduate School of Medicine, Kyoto, Japan
[3]Department of Neurosurgery, Kanazawa University Hospital, Kanazawa, Japan

Cell replacement therapy holds great promise as a means of treating neurological disorders, including Parkinson's disease. However, one of the major obstacles to the success of this treatment is the low survival rate of grafted cells, which probably results from mechanical damage, acute inflammation, and immunological rejection. To overcome this problem, we investigated the effect of different types of extracellular matrix (ECM) on the survival and differentiation of embryonic stem (ES) cell-derived neural precursor cells (NPCs). We tested materials from natural sources, including collagen, ornithine/laminin, and growth factor-reduced Matrigel (gfrMG), as well as the synthetic biomaterial PuraMatrix, which consists of self-assembling polypeptides. GfrMG efficiently supported cell survival, migration, and neurite outgrowth in vitro and promoted proliferation of grafted cells in vivo, resulting in larger graft volume and an increase in the number of TH-positive dopaminergic neurons in the graft. GfrMG did not induce dopaminergic differentiation directly; rather, it reduced the invasion of pan-leukocytic CD45-positive cells into the graft. Insofar as the inflammatory or immune response in the host brain inhibits neuronal differentiation of grafted NPCs, gfrMG may increase the number of TH-positive cells by suppressing this effect. Thus, gfrMG appears to provide a suitable scaffold that supports survival and differentiation of NPCs. However, because it is derived from mouse sarcomas, a human-derived matrix or synthetic biomaterial must be developed for clinical applications.

Key words: extracellular matrix; transplantation; inflammation; embryonic stem cells

With recent advances in biotechnology, cell replacement therapy is becoming a promising treatment option for neurological diseases (Lindvall et al., 2004; Goldman, 2005). For example, fetal nigral cell transplantion into patients with Parkinson's disease results in neurological improvement in younger patients (Freed et al., 2001; Olanow et al., 2003). However, because of a shortage of fetal cell supply, stem cells are expected as alternative donor cells. Embryonic stem (ES) cells can be differentiated into neural precursor cells (NPCs) by the stromal cell-derived inducing activity (SDIA) method, which involves in vitro culture on a mouse PA6 stromal cell feeder layer. This technique effectively produces dopaminergic (DA) neurons that can be used for transplantation (Kawasaki et al., 2000).

One current problem with cell transplantation is the low rate (5–20%) of graft survival. Most cell death occurs during the first few days following transplantation as a result of acute inflammation or immune response, trophic factor withdrawal, oxidative stress, excitotoxicity, hypoxia, and anoikis (Zawada et al., 1998; Sortwell et al., 2000; Emgard et al., 2003). Anoikis is a type of apoptosis that is triggered by detachment from the extracellular matrix (ECM) and neighboring cells, as occurs in cell dissociation (Frisch and Francis, 1994). Thus, for successful transplantation, we must reconstruct the three-dimensional extracellular environment of grafted cells, which is composed of ECM, cytokines, and neighboring cells.

Biomaterials can support the development of cells and tissues by providing a suitable microenvironment for cell attachment, proliferation, and ECM deposition (Lutolf and Hubbell, 2005). Animal-derived biomaterials such as collagen, laminin, and polyglycosaminoglycans and basement membrane materials such as Matrigel (MG) have been widely used in cell culture applications (Lelievre et al., 1998). Collagen is the most abundant

The first two authors contributed equally to this work.

Contract grant sponsor: JSPS Grant-in-Aid for Scientific Research; Contract grant sponsor: Kobe Cluster MEXT; Contract grant sponsor: Leading Project from the MEXT of Japan; Contract grant sponsor: Takeda Science Foundation.

*Correspondence to: Jun Takahashi, MD, PhD, Department of Biological Repair, Institute for Frontier Medical Sciences, Kyoto University, 53 Shogoin kawahara-cho, Sakyo-ku, Kyoto 606-8507, Japan.
E-mail: jbtaka@frontier.kyoto-u.ac.jp

Received 28 March 2009; Revised 19 June 2009; Accepted 30 June 2009

Published online 22 September 2009 in Wiley InterScience (www.interscience.wiley.com). DOI: 10.1002/jnr.22223

protein (by weight) in animals, accounting for 30% of all protein in mammals. It is the major component of connective tissue, tendon, ligaments, and cornea and forms the matrix of bones and teeth (Patino et al., 2002b). Collagen gel can be used both as a carrier for cell transplantation (Weinand et al., 2007) and as a cell infiltration matrix to induce regeneration and remodeling in vivo (Patino et al., 2002a). MG is a solubilized basement membrane extracted from the Engelbreth-Holm-Swarm (EHS) mouse sarcoma. Its major component is laminin, and it also contains collagen IV (Col IV), heparin sulfate proteoglycans, entactin, and nidogen (Kleinman et al., 1986). MG has been used successfully in transplantation experiments, in a cardiac infarction model to restore heart geometry and function (Kutschka et al., 2006; Zhang et al., 2006), and in an arterial injury model to promote angiogenesis and endothelial proliferation (Xiao et al., 2006).

Artificial biomaterials such as porous, biodegradable polymer scaffolds allow formation of complex three-dimensional tissues during differentiation and provide physical cues for cell orientation and spreading and thus may support survival of grafted stem cells (Lutolf and Hubbell, 2005). Nano-structured porous PLLA (poly-L-lactic acid) has been used successfully as a scaffold in nerve tissue engineering (Yang et al., 2004), and L1-Fc-coated polyglycolic acid (PGA)-chitosan conduits provide a supportive canal to guide regeneration and remyelination of injured nerves (Xu et al., 2004; Bhang et al., 2007). Recently, a synthetic, self-assembling RADA16 peptide hydrogel scaffold, PuraMatrix (PM), was shown to support the adhesion, survival, and differentiation of adult mouse neural stem cells (Gelain et al., 2006).

To find an implantable matrix that supports survival and differentiation of ES cell-derived NPCs, we compared the supportive effects of different types of matrices: Col IV, poly-L-ornithine/laminin (OL), MG, and PM in vitro. Col IV and laminin are present in the basement membrane and have been implicated in development of the neuromuscular junction and in axonal growth (Hubert et al., 2008). They are also present in fractones, extravascular basal lamina structures involved in neurogenesis during both development and adulthood (Kerever et al., 2007). In addition, both are major components of MG. The original formulation of MG contains growth factors such as fibroblast growth factor-2 and insulin-like growth factor-1, but, to try to examine the effect of the matrix itself, we used growth factor-reduced MG (gfrMG) in the present study. Furthermore, we investigated the in vivo effect of gfrMG on survival and neuronal differentiation of the grafted NPCs.

MATERIALS AND METHODS

Biomaterials Used

Both natural and synthetic biomaterials were used. The natural biomaterials we used included gfrMG (BD Biosciences, San Jose, CA), Col IV (BD Biosciences), poly-L-ornithine (Sigma-Aldrich, St. Louis, MO), and laminin (Collaborative Biomedical Products). As a synthetic material, we used PM (3-D Matrix Japan). NPCs were not able to survive when cultured on glass slides, so we coated slides with 0.1% gelatin (Gel; Sigma-Aldrich) as a control.

Induction of Neural Differentiation of ES Cells

EB5 and G4-2 cells (both mouse ES cell lines were kind gifts from Dr. Hitoshi Niwa, RIKEN Center for Developmental Biology, Kobe, Japan) carry the blasticidin S-resistance gene driven by the Oct3/4 promoter, which is active in the undifferentiated state. Cells were maintained in medium containing 20 μg/ml blasticidin S to eliminate differentiated cells. G4-2 cells, which were derived from EB3 cells, also carry green fluorescence protein (GFP) under the control of the CAG promoter, which allowed us to identify GFP-positive donor cells grafted into host brains in our in vivo studies. Both EB3 and EB5 cells are subclones of E14tg2a ES cells, so these two cell lines have identical genetic backgrounds (Matsuura et al., 2006; Ogawa et al., 2007). G4-2 cells were used for transplantation and EB5 cells for the remaining experiments. Undifferentiated mouse ES cells were maintained on gelatin-coated (0.1%) 6-cm dishes in Glasgow modified Eagle's medium (G-MEM; Gibco-Invitrogen, Grand Island, NY) supplemented with 1% fetal calf serum (FCS; JRH), 10% knockout serum replacement (KSR; Gibco-Invitrogen), 2 mM glutamine, 0.1 mM nonessential amino acids, 1 mM pyruvate, 0.1 mM 2-mercaptoethanol (2-ME), and 2,000 U/ml leukemia inhibitory factor (LIF; Gibco-Invitrogen). For differentiation, ES cells were treated by the SDIA method as previously reported (Kawasaki et al., 2000). Briefly, ES cells (500 cells/10-cm dish) were cocultured on a layer of PA6 cells (mouse calvarial stromal cells) in differentiation medium (GMEM supplemented with 10% KSR, 2 mM L-glutamate, 0.1 mM nonessential amino acids, 1 mM pyruvate, and 0.1 mM 2-ME). Undifferentiated ES cells were allowed to differentiate into colonies for 8 days before re-replating on the matrices for both in vitro studies and in vivo transplantation.

Immunofluorescence Study

For immunofluorescence of cultured cells, cells were fixed with 4% paraformaldehyde (PFA) in phosphate-buffered saline (PBS) for 15 min. For immunofluorescence of tissue, mice that had undergone transplantation were placed under deep anesthesia with pentobarbital, then perfused transcardially with cold PBS (pH 7.4), followed by cold 4% PFA (pH 7.4). The brain was removed and kept in 4% PFA overnight, then immersed into 30% sucrose until the brain sank. Brains were frozen in OCT compound (Tissue-Tek) and cut with a microtome (Leica CM 1850) at 20 μm thickness and collected in PBS. The free-floating method was used for staining the brain sections. For immunofluorescence of brain slices at 24 hr, the slices were immediately adhered to a glass slide, and staining was performed on the slide. The brain sections and fixed cells were incubated in PBS containing 5% preimmune donkey serum and 0.3% Triton X-100 (PBST-DS) for 30 min, then in primary antibodies in PBST-DS at optimal dilution overnight at 4°C. After three washes with PBS

containing 0.3% Triton X-100 (PBST), the slices were incubated for 2 hr at room temperature in Alexa Fluor 488- or 546-conjugated secondary antibodies (Invitrogen) diluted 1:600 in PBST-DS. Brain sections were transferred onto glass slides with 100 mM Tris, pH 8.5, containing 25% glycerol, 10% polyvinyl alcohol (Air Products), and 2.5% 1,4-diazobicyclo-[2.2.2]-octane (Sigma-Aldrich). PeraFluor (Beckman Coulter) was used as a mounting medium.

Primary antibodies used were as follows (mo, mouse monoclonal; rb, rabbit polyclonal; sh, sheep polyclonal): mo or rb anti-β-tubulin, 1:300 (Tuj1; Covance Research Products, Richmond, CA); mo antinestin, 1:200 (Chemicon); rb anti-GFAP, 1:300 (Chemicon, Temecula, CA); rb or sh anti-tyrosine hydroxylase, 1:100 (TH; Chemicon); rb anti-Ki67, 1:500 (Novocastra); rat anti-CD45, 1:300 (IBL-3/16; Gene Tex, Inc.); and rb or rat antigreen fluorescent protein, 1:150 or 300 (GFP; MBL). For nuclear staining, 200 ng/ml of 4,6-diamidino-2-phenylindole (DAPI) was added to the final wash. After immunofluorescence, the number and percentage of immunoreactive cells were evaluated randomly and blindly using a Fluoview FV300 laser confocal microscope (Olympus Optical Co.) or a BZ-8000 microscope (Keyence Co.) with the settings unchanged between samples for each antibody and treatment. For in vivo experiments, the number of immunoreactive cell profiles was quantified in every sixth section throughout the graft. The total number of immunoreactive profiles in each graft was then estimated by using Abercrombie's method.

Effect of ECM on Cell Survival, Neurite Outgrowth, Cell Migration, and Dopaminergic Differentiation

Eight-well glass chamber slides (Falcon) were coated with the following ECM material: 0.1% Gel, 10 μl/cm^2 Col IV, 50 μg/ml poly-L-ornithine, 5 μg/ml laminin, 5 μl/cm^2 gfrMG, 0.2% PM overnight. The colonies differentiated from EB5 cells by the SDIA method for 8 days (8-day SDIA colonies, hereafter) were detached from the PA6 feeder layer using the papain dissociation system (Worthington Biochemical Corporation), according to the manufacturer's protocol. To examine cell survival, 8-day SDIA colonies were gently dissociated using Accumax (Inovate Cell Technologies) and grown on precoated chamber slides (10^5 cells/cm^2) for 3 days. Cultures were subjected to nuclear staining with DAPI, and the number of surviving cells with large and oval nuclei was counted (n = 40 fields of 0.036 mm^2 for each matrix). To examine neurite outgrowth, colonies were cultured on each matrix (3–10 colonies per well) in conditioned neurobasal medium from PA6 cells supplemented with 2% B27 (Gibco-BRL), 0.5 mM L-glutamine (Sigma-Aldrich) for 6 days and subjected to immunofluorescence with an anti-Tuj1 antibody. First, the number of the extending neurites from each colony was counted at 100–200 μM from the edge (n = 10 for each). Then, a polygon connecting the tips of all the neurites was drawn around each colony and the area measured (Gel; n = 36 colonies, Col IV; n = 21, OL; n = 45, gfrMG; n = 39, PM; n = 48). To evaluate cell migration, colonies were cultured on each matrix (3–10 colonies per well) for 6 days in conditioned differentiation medium after 24 hr of incubation with confluent PA6 cells, then subjected to immunofluorescence with anti-nestin or anti-GFAP antibodies. The distance of positive cells from the center of the colony was measured for the most distant 10 cells of each colony (nestin: n = 8, 9, 29, 22, 27 colonies; GFAP: n = 12, 10, 22, 12, 9 for Gel, ColIV, OL, gfrMG, and PM, respectively). To investigate DA differentiation, colonies were incubated for 6 days with conditioned neurobasal medium from 24-hr confluent PA6 cell culture supplemented with 2% B27, 0.5 mM l-glutamine on each matrix (3–10 colonies per well). Colonies were subjected to immunofluorescence with an anti-TH antibody, and the number of positive cells was counted for each colony (Gel; n = 8 colonies, Col IV; n = 8, OL; n = 20, gfrMG; n = 22, PM; n = 17).

Transplantation of Mouse ES Cell-Derived NPCs

Wild-type 8-week-old C57BL/6CrSlc adult male mice (SLC, Shizuoka, Japan) weighing 18–22 g were used. Animal experiments were performed in accordance with the Guidelines for Animal Experiments at Kyoto University. All surgical procedures were performed with animals under deep anesthesia with sodium pentobarbital (50 mg/kg). Eight-day SDIA colonies generated from G4-2 ES cells were collected by centrifugation, and one-tenth of each sample was dissociated for cell counting. The remaining colonies were adjusted to a density of 1 × 10^5 cells/μl in gfrMG or differentiation medium (control). Each mouse received a stereotactic injection of 2 μl (1 μl/min) of cells using a 26-gauge needle into the bilateral striatum (from the bregma: A +0.5, R or L +2.0, V +3.0, incisor bar 0; gfrMG = right side, control = left side). Animals were sacrificed 24 hr, 72 hr, or 4 weeks posttransplantation. Graft volume was measured in Adobe Photoshop CS3. In indicated cases, immunosuppression was induced by intraperitoneal administration of cyclosporine A (Calbiochem, La Jolla, CA; 0.2 mg/ml), initiated 3 days in advance of transplantation and continued until the day of sacrifice. With this procedure, plasma cyclosporine A levels were measured at 297 ± 55 ng/ml after 4 weeks (n = 7).

TUNEL Staining

Cell death was determined by a TdT-mediated dUTP nick-end labeling (TUNEL) assay using the In Situ Cell Death Detection Kit (Roche), according to the manufacturer's instructions. TUNEL staining of grafts with or without gfrMG was performed with brain slices 24 or 72 hr after transplantation. TUNEL-positive cells with condensed chromatin were scored as apoptotic cells and were counted manually with an Axioplan 2 microscope (Zeiss).

Statistical Analysis

Statistical analysis was performed with a commercially available software package (Statview 5.0; SAS Institute Inc., Cary, NC). Data were tested by the Student's *t*-test or one-way ANOVA followed by Dunnet's or Tukey's post hoc analysis. Differences were considered statistically significant at $*P < 0.05$, **0.001, or ***0.0001. Data values are presented as the means ± SEM. All results were derived from three to seven independent experiments.

RESULTS

Cell Survival and Neurite Elongation on ECM Materials

To compare the supportive effects of ECM materials, we investigated the survival, neurite elongation, migration, and differentiation of ES cell-derived NPCs grown in vitro on these matrices. When mouse ES cells are cultured on PA6 stromal cells (SDIA method), they differentiate into a neural lineage. Previous data showed that the majority of cells are stained with either the neuronal marker Tuj1 or the neural precursor marker nestin on day 8 (Kawasaki et al., 2000). To evaluate cell survival on different matrices, 8-day SDIA colonies were dissociated and replated onto culture dishes coated with Gel, Col IV, OL, gfrMG, or PM. On day 3, we counted the number of surviving cells, and found that gfrMG most efficiently supported the survival of NPCs (Fig. 1A).

Next, 8-day SDIA colonies were replated on these matrices and cultured for 6 days. Within 24 hr, neurites began to grow out and extend radially. After 6 days, dense Tuj1-positive fibers were observed (Fig. 1C). Thick fiber bundles were frequently observed in colonies grown on OL and gfrMG, whereas fibers of colonies grown on PM were thin and separated. The numbers of extending neurites were 5 ± 1.1, 6 ± 1.3, 185 ± 21.4, 258 ± 15.2, and 201 ± 8.3 on Gel, Col IV, OL, gfrMG, and PM, respectively. To evaluate further the degree of neurite elongation, we drew a polygon linking all the neurite tips for each colony and measured the area covered. The average area was larger in colonies grown on OL or gfrMG compared with other matrices tested (Fig. 1B).

We also examined cell migration on each matrix. As the cells contained and differentiated from the colonies were NPCs (nestin$^+$), neurons (Tuj1$^+$), astrocytes (GFAP$^+$), and very few oligodendrocytes, we performed immunostaining against nestin, Tuj1, and GFAP and evaluated migration of NPCs and astrocytes. Immunofluorescence of colonies grown for 6 days on gfrMG revealed nestin-positive cells (NPCs; green in Fig. 1D) and GFAP-positive cells (astrocytes, green in Fig. 1F) that had migrated out from the colony. The average distance of the 10 cells migrating farthest from the colony center was greater for OL and gfrMG compared with other matrices tested, and NPCs tended to migrate farther than astrocytes (Fig. 1E,G).

Finally, as the SDIA method induces predominantly DA neurons, we evaluated the number of the cells that expressed the DA neuron marker TH in each colony following culture on different matrices for 6 days. TH-positive cells were observed (Fig. 1H), but there was no significant difference in the number of the TH-positive cells per colony area (Fig. 1I).

Transplantation of ES Cell-Derived NPCs With gfrMG

Because our in vitro results indicated that gfrMG supported survival, neurite elongation, and migration of ES cell-derived NPCs, we transplanted NPCs with gfrMG to evaluate the effect of this matrix in vivo. In analysis of DA neuron differentiation and Parkinsonian behavior, 6-hydroxydopamine-lesioned animals are often used. However, in this study, we used unlesioned mice with intact striatum as graft recipients, because we wished to examine graft survival, not behavioral recovery. In addition, depletion of DA neurons might promote DA neuronal differentiation and survival (Nishino et al., 2000). We wished to avoid individual difference of the depletion effect between lesioned mice. As donor cells, we used G4-2 ES cells, which are genetically modified to express GFP, to monitor surviving transplanted cells by green fluorescence. We subjected ES cells to SDIA treatment for 8 days to induce neuronal differentiation, then transplanted the cells with (left striatum) or without (right striatum) gfrMG into the mouse brain. To examine the effect of immune response by the host brain, we performed grafts with (n = 7) or without (n = 5) immunosuppression (cyclosporine A; CsA).

After 4 weeks, the grafted cells survived in all animals, and some expressed the DA neuron marker TH (Fig. 2A–C). The average volume was significantly larger in the graft with gfrMG both in the presence and in the absence of CsA (Fig. 2D,E, left). The average number of TH-positive cells in each graft was also significantly larger when NPCs were transplanted with gfrMG than those observed in control grafts (Fig. 2D,E, middle). However, there was no significant difference between grafts with or without gfrMG in the number of TH-positive cells per unit volume (Fig. 2E, right). These results indicate that gfrMG supports the survival and/or proliferation of the grafted NPCs, which leads to an increased number of DA neurons in the graft. They also suggest that induction of TH-positive cells is influenced by immune response of the host brain.

GfrMG induced neurite elongation and also migration of NPCs and NPC-derived astrocytes in vitro. However, these was no substantial neurite extension or cell migration from the graft into the host brain irrespective of whether or not gfrMG was used in vivo.

Effect of gfrMG on Grafted Cells In Vivo

To investigate why gfrMG increased the volume of the graft, we examined cell death and proliferation of the grafted cells. Previous reports indicated that most cell death occurs during the first few days following transplantation (Sortwell et al., 2000), so we grafted 8-day SDIA colonies into the mouse striatum and counted the number of apoptotic cells in the graft after 24 or 72 hr (n = 3 in each group) by TUNEL staining (Fig. 3A). There was no significant difference in graft volume in mice that received cell transplantation with or without gfrMG at either 24 or 72 hr (0.19 ± 0.10 and 0.16 ± 0.03 mm^3 at 24 h; 0.28 ± 0.20 and 0.28 ± 0.08 at 72 hr for gfrMG and control, respectively). TUNEL-positive cells were more frequently observed in the graft with gfrMG at 24 hr, but the difference became insignif-

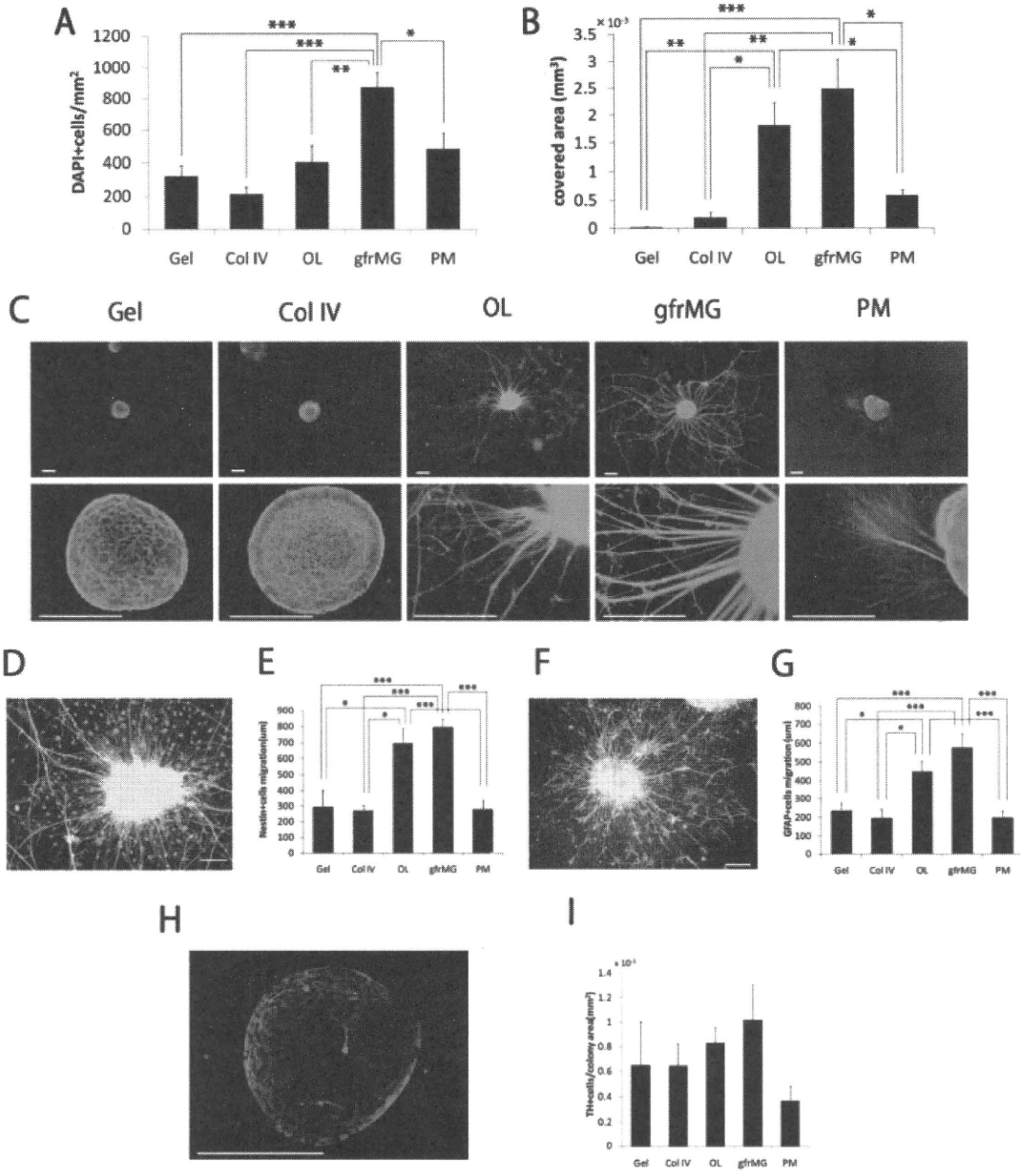

Fig. 1. In vitro effects of different matrices. Cell survival at day 3 (**A**) was most enhanced with gfrMG ($*P < 0.05$, $***P < 0.0001$ compared with other matrices). Immunostaining for Tuj1 in 8-day SDIA colonies grown for 6 days on different matrices shows neurite outgrowth from colonies (**C**). OL and gfrMG promoted neurite outgrowth more than other matrices (**B**; $*P < 0.05$, $**P < 0.001$, $***P < 0.0001$ compared with other matrices). Immunostaining for nestin (green in **D**), GFAP (green in **F**), and Tuj1 (red in D,F) in 8-day SDIA colonies grown for 6 days on gfrMG shows that nestin-positive NPCs and GFAP-positive astrocytes migrated outward from the colony. Migration of nestin (**E**)- and GFAP (**G**)-positive cells was increased on OL and gfrMG compared with other matrices ($*P < 0.05$, $**P < 0.001$, $***P < 0.0001$ compared with other matrices). On day 6, the colonies grown on gfrMG gave rise to TH-positive DA neurons (red in **H**), but there was no significant difference in the number of TH-positive cells per colony area (mm^3) among the different matrix conditions (**I**). Scale bars = 200 μm in C,H; 100 μm in D,F.

icant at 72 hr (Fig. 3C). These results suggest that gfrMG promotes immediate death of grafted NPCs or reduces phagocytosis of apoptotic cells. The number of proliferating cells in the graft was evaluated by immunofluorescence for proliferation antigen Ki67 72 hr (n = 6) and 4 weeks (n = 4) after transplantation (Fig. 3B). Ki67-positive cells were more frequently observed in the graft with gfrMG at 72 hr, but after

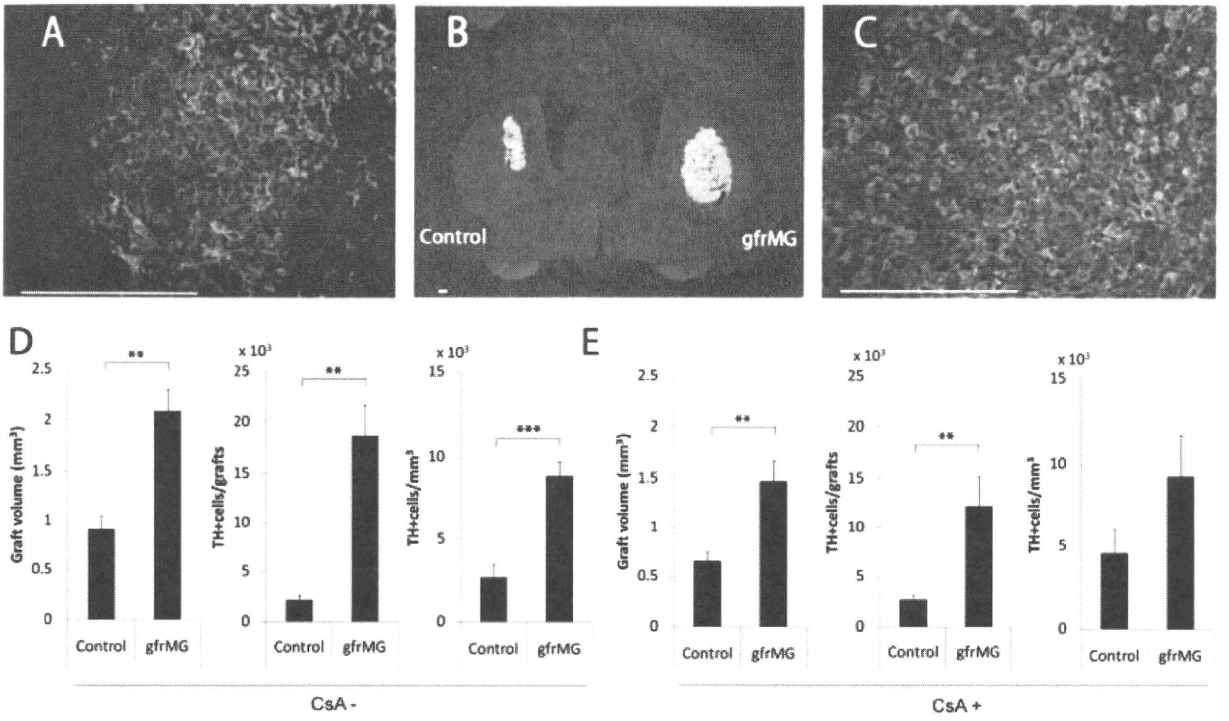

Fig. 2. Transplantation of ES cell-derived NPCs with or without gfrMG. Mouse ES cell-derived NPCs were grafted with (B, right, **C**) or without (**A,B**, left) gfrMG. Immunohistochemistry 4 weeks after transplantation shows that grafted cells (green in A–C) survived in the striatum and that some differentiated into TH-positive DA neurons (red in A–C). **D,E:** The graft volume and the number of TH-positive cells per graft were significantly larger with gfrMG, irrespective of immunosuppression (n = 5, CsA in D; n = 7, CsA^+ in E, $^{**}P < 0.001$, $^{***}P < 0.0001$). However, the number of TH-positive cells per volume did not differ between grafts with or without gfrMG when the mice were immunosuppressed (E, right). Scale bars = 200 μm.

4 weeks the frequency was much lower and the difference became insignificant (Fig. 3D). These results suggest that gfrMG promotes proliferation of the surviving cells.

Next, we investigated the effect of gfrMG on inflammatory or immune responses of the host brain. We grafted 8-day SDIA colonies into the mouse striatum without immunosuppression, and then invasion of inflammatory or immune cells into the graft was evaluated by immunofluorescence for the pan-leukocytic marker CD45, which is expressed by microglia, macrophages, and lymphocytes (Fig. 4A; n = 3 in each group). At 24 hr after transplantation, only a few CD45-positive cells were detected in NPC grafts with gfrMG, suggesting that gfrMG prevented invasion of inflammatory cells into the graft. However, after 72 hr or 4 weeks, the number of the invading cells gradually increased, and the numbers did not differ significantly between animals with or without gfrMG (Fig. 4B).

DISCUSSION

Here, we sought to identify an implantable matrix that supports survival and differentiation of ES cell-derived NPCs. We have shown that gfrMG increased the graft volume and the number of DA neurons in the graft 4 weeks after transplantation. Previous study with bone marrow-derived mesenchymal stem cells showed that MG supported graft survival more efficiently than collagen I, PM, or control injections with PBS. Moreover, only MG could support cell survival for up to 5 months (Cao et al., 2007). The possible mechanisms for the supportive effect of gfrMG include rescue of dying cells, promotion of cell proliferation, blockage of invading inflammatory or immunological cells, and promotion of neuronal differentiation. Although gfrMG has fewer growth factors than conventional MG, the supportive effect may result not only from better scaffolding but also from growth factors still present in gfrMG. Indeed, growth factors present in conventional MG appear to act on other types of cells, including olfactory ensheathing cells (Tisay and Key, 1999), Schwann cells (Yoshino et al., 1990), and bone marrow stromal cells (Qian and Saltzman, 2004).

In initial in vitro experiments, we compared the effects of biological and synthetic matrices, including Col IV, OL, gfrMG, and PM, on mouse ES cell-derived NPCs. We showed that gfrMG most efficiently supported cell survival (Fig. 1A). OL and gfrMG promoted neurite elongation and migration of NPCs and

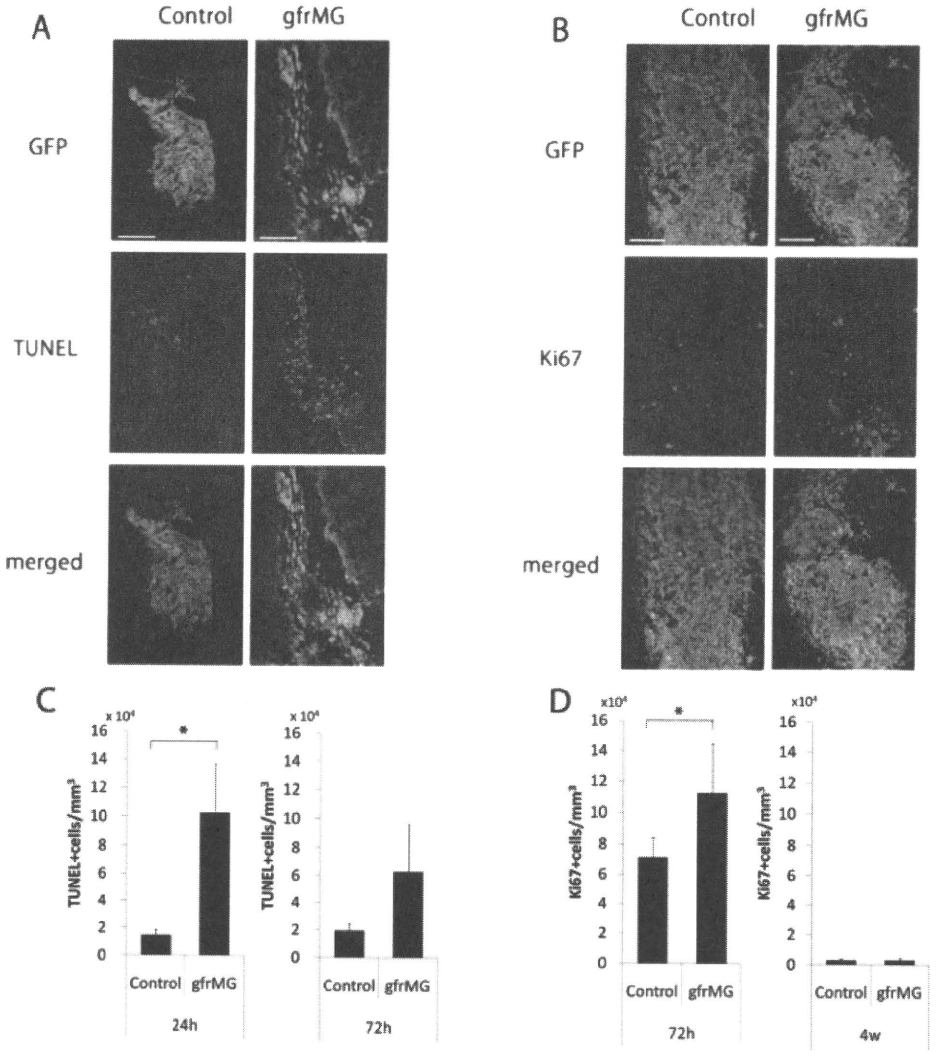

Fig. 3. Cell death and proliferation of NPCs in the graft. Grafted NPCs (GFP, green in **A,B**) in the striatum underwent apoptosis (TUNEL, red in A; 24 hr after transplantation), and surviving cells proliferated (Ki67, red in B; 72 hr). **C:** GfrMG increased the number of TUNEL-positive cells in the graft at 24 hr, but the difference became insignificant at 72 hr (n = 3 in each group, $*P < 0.05$). **D:** GfrMG increased the number of Ki67-positive cells in the graft at 72 hr, but the number decreased by 4 weeks, and the difference became insignificant (n = 6 at 72 hr; n = 4 at 4 weeks, $*P < 0.05$). Scale bars = 100 μm.

NPC-derived astrocytes more than other matrices (Fig. 1B–G). These results suggest that gfrMG provides the best environment for NPCs. However, in our in vivo study, more TUNEL-positive cells were detected in the graft with gfrMG than in the control graft at 24 hr (Fig. 3A,B). It is possible that shear stress and/or hypoxic conditions were enhanced by gfrMG, which might cause immediate cell death. Another possibility is that gfrMG reduced the immediate phagocytosis of apoptotic cells (Kurosaka et al., 2003) by inhibiting the invasion of host-derived macrophages (Fig. 4). Thus it is possible that the apoptotic cells were swept out in the control graft while they remained in the graft with gfrMG. However, the exact mechanism must be explored. Similarly, in spite of a supportive effect of gfrMG in vitro, gfrMG failed to induce neurite extension or cell migration from the graft into the host brain. It is probably because that gfrMG could not diffuse into the host brain and could not work as a scaffold to support neurite extension or cell migration.

At day 3, Ki67-positive proliferating cells were more frequently observed in grafts with gfrMG, suggesting that gfrMG promotes proliferation of NPCs. MG has been reported to promote expansion of human ES cell-derived NPCs in culture more than collagen and fibronectin (Ma et al., 2008). Thus, our in vitro data showing increased cell survival on gfrMG may reflect a supportive effect of gfrMG on cell proliferation.